

## Seismic Performance Evaluation of Irregular Auditorium Building based on ASCE 41-23

Ananda Elnish Fiqhunissa<sup>1</sup>, Iman Satyarno<sup>1\*</sup>, Angga Fajar Setiawan<sup>1</sup>,  
Mariyana Aida Ab Kadir<sup>2,3</sup>, Muhamad Fauzi Darmawan<sup>1</sup>

<sup>1</sup>Department of Civil and Environmental Engineering, Gadjah Mada University, Yogyakarta, INDONESIA

<sup>2</sup>Department of Structure and Material, Faculty of Civil Engineering, University of Technology Malaysia, Johor Bahru, MALAYSIA

<sup>3</sup>Institute of Noise and Vibration, University of Technology Malaysia, Kuala Lumpur, MALAYSIA

\*Corresponding author: [imansatyarno@ugm.ac.id](mailto:imansatyarno@ugm.ac.id)

SUBMITTED 20 May 2024 REVISED 28 June 2024 ACCEPTED 2 August 2024

**ABSTRACT** This study discusses the seismic performance evaluation of an irregular auditorium building. The building is an educational facility which has roof span up to 46 meters, column height up to 10 meters, beam span up to 15 meters, cantilever up to 6.50 meters, 2 inclined columns with the angle up to 54.72°, and 1 transfer column with 1 transfer beam. The evaluation process was carried out using Tier 3 method with linear dynamic procedure which consisted of Response Spectrum Analysis (RSA) and Linear Time History Analysis (LTHA) according to ASCE 41-23 using SAP2000 subjected to short ( $S_s$ ) and long ( $S_l$ ) period of earthquakes. The building is designed to Risk Category IV, which the target performance levels for structural components are Immediate Occupancy (IO) for Basic Safety Earthquake 1 for New Building (BSE-1N) and Life Safety (LS) for Basic Safety Earthquake 2 for New Building (BSE-2N). Even though the building had a torsional strength irregularity, the percentage of components with a Demand-Capacity Ratio value that did not meet the requirements was 9.87% of the total components; hence the linear procedure was assumed to be still applicable. Analyses showed that the average acceptance criteria ratio of the components with the RSA method was lower than with the LTHA method but the percentage of the components with acceptance criteria ratio exceeding 1 using RSA method was higher than using the LTHA method. In addition, the results indicated that the average performance level of the components was IO for BSE-1N and LS for BSE-2N, which both results had met the expected performance level targets. However, the maximum performance level of the components did not meet the IO performance level target for BSE-1N and did not meet the LS performance level target for BSE-2N.

**KEYWORDS** New irregular building, Tier 3 evaluation, Linear dynamic procedure, Response spectrum analysis method, Linear time history analysis method

© The Author(s) 2024. This article is distributed under a Creative Commons Attribution-ShareAlike 4.0 International license.

### 1 INTRODUCTION

Indonesia is one of the most seismically active regions globally due to its location on the Pacific Ring of Fire, where several tectonic plates meet and interact. This tectonic setting results in frequent and sometimes devastating earthquakes. Historical records show that Indonesia has experienced numerous significant seismic events, which have had profound effects on its population and infrastructure. The 2004 Indian Ocean earthquake and tsunami, one of the deadliest natural disasters in recorded history, caused widespread devastation and loss of life (Ramalanjaona, 2011). More recently, the 2006 Yogyakarta earthquake resulted in thousands of fatalities and extensive damage to buildings and infrastructure (Nurwihastuti et al., 2014). The 2018 Sulawesi earthquake, followed by a devastating tsunami, further highlighted the vulnerability of Indonesian cities to seismic activity (Harnantaryi et al., 2020). These events have underscored the critical need for robust seismic design and evaluation standards to mitigate the impacts of future earthquakes. The frequent seismic activity in Indonesia necessitates ongoing

research and the implementation of advanced engineering practices to enhance the resilience of buildings and infrastructure in this highly earthquake-prone region.

Irregular buildings, which are characterized by non-uniform mass, stiffness, or geometry, pose significant challenges in seismic design due to their complex behavior under earthquake loads. These structures are particularly susceptible to damage during seismic events because their irregularities can lead to uneven distribution of seismic forces and induce torsional movements (Alecci and Stefano, 2019). Research indicates that the seismic response of irregular buildings is more severe compared to regular buildings (Paul et al., 2023). For example, Hussein et al. (2019) demonstrated that torsional irregularities could result in excessive displacement and stress concentrations, leading to potential structural failures. Similarly, Nady et al. (2022) found that plan and vertical irregularities significantly increased the seismic demands on structures, causing

higher potential for damage and collapse. These studies highlight the critical need for special consideration and advanced analysis methods when designing and evaluating irregular buildings. Ensuring the seismic resilience of such structures requires a thorough understanding of their unique dynamic characteristics and the implementation of tailored seismic performance evaluation methods.

The American Society of Civil Engineers (ASCE) 41-23 standard provides comprehensive guidelines for the seismic evaluation and retrofit of existing buildings. This standard includes various methods for assessing the seismic performance of buildings, such as nonlinear static procedures, nonlinear dynamic procedures, and linear dynamic procedures. These methods are essential for predicting the potential seismic response of structures and for designing appropriate retrofitting measures to enhance their performance under earthquake loads. The nonlinear static procedure, also known as pushover analysis, involves applying a gradually increasing lateral load to the building model to identify its capacity and potential failure modes (ASCE, 2023). Nonlinear dynamic procedures, on the other hand, involve detailed time-history analysis using recorded or simulated ground motions to capture the building's dynamic response (ASCE, 2023). Linear dynamic procedures, including Response Spectrum Analysis (RSA) and Linear Time History Analysis (LTHA), provide simplified yet effective means of evaluating the seismic performance of buildings. These methods, when applied in accordance with ASCE 41-23, offer valuable insights into the behavior of irregular buildings under seismic loads and help engineers design more resilient structures (Chandrakar and Bokare, 2017).

The RSA and LTHA are crucial techniques for understanding the seismic behavior of irregular buildings. RSA provides a simplified approach to estimate the maximum response of a structure using predefined response spectra, which represent the peak response of a single-degree-of-freedom system to various ground motion inputs (Manoj and Varghese, 2022). This method is particularly useful for preliminary design and assessment, as it offers a quick and reliable means of evaluating seismic demands. However, it may not fully capture the complex dynamic interactions in irregular buildings. In contrast, LTHA involves simulating the building's response to actual earthquake ground motions over time, providing a more detailed evaluation of its seismic performance (Aysha, 2021). This method can reveal critical insights into the building's behavior under real seismic conditions, including potential failure modes and the effectiveness of seismic design measures. Evaluating both RSA and LTHA is essential because they offer different perspectives on the seismic performance of irregular buildings. By comparing these methods, engineers can identify potential

weaknesses in the design and implement more effective retrofitting strategies to ensure the resilience of irregular structures.

The object used in this research is an auditorium building which has a total of 4 stories. This building has complex floor plans and roof structures. In addition, the building also has large dimension of components, such as roof span up to 46 meters, column height up to 10 meters, beam span up to 15 meters, and cantilever up to 6.5 meters. In order to support the wide cantilevers, the building has 2 inclined columns with an angle up to  $54.72^\circ$ . With these complex structures and large structural components, auditorium building is classified as an irregular building with torsional strength irregularity. Buildings that are categorized as irregular buildings need to be evaluated in more detail to ensure that all structural components of the building can maintain their performance before and after an earthquake. Besides that, the analysis procedures that are allowed to be applied also depend on the presence or absence of irregularities in the building. Therefore, before analyzing and evaluating the irregular structures, it is necessary to determine what irregularities are present in the building and to figure out what aspects need to be considered as the consequences of the irregularities.

Despite significant advancements in seismic performance evaluation methods, there remains a knowledge gap in understanding the complex behavior of irregular buildings under seismic loads. Previous studies have primarily focused on regular structures or specific types of irregularities, highlighting the need for more comprehensive research on various irregular configurations. The objective of this study is to bridge this gap by evaluating the seismic performance of an irregular auditorium building based on ASCE 41-23 guidelines. This research aims to provide insights into the effectiveness of RSA and LTHA in predicting the seismic response of irregular buildings. By conducting detailed analyses and comparisons, this study seeks to enhance our understanding of the unique challenges posed by irregular buildings during earthquakes and contribute to the development of more robust seismic design and retrofitting strategies. Ultimately, this research aims to improve the resilience of irregular buildings, thereby reducing the risk of damage and loss of life in future seismic events.

## 2 METHODS

The approach used in this research was a numerical approach with macro model (general model) using frame elements for beams and columns and shell elements for slabs in SAP2000 software. Since the building is classified as a new building, the evaluation process was carried out using Tier 3 method. Based on ASCE 41-23, Tier 3 is typically employed for new buildings or build-

Table 1. Material properties.

Material	Compressive strength ( $f'_c$ , MPa)	Modulus of elasticity ( $E_c$ or $E_s$ , MPa)	Grade type	Yield strength ( $f_y$ , MPa)	Ultimate strength ( $f_u$ , MPa)
Concrete	35	27805.58	-	-	-
Rebar	-	200000	60	420	525
Stirrup rebar	-	200000	40	280	390
Steel profile pipe	-	200000	A36	250	400

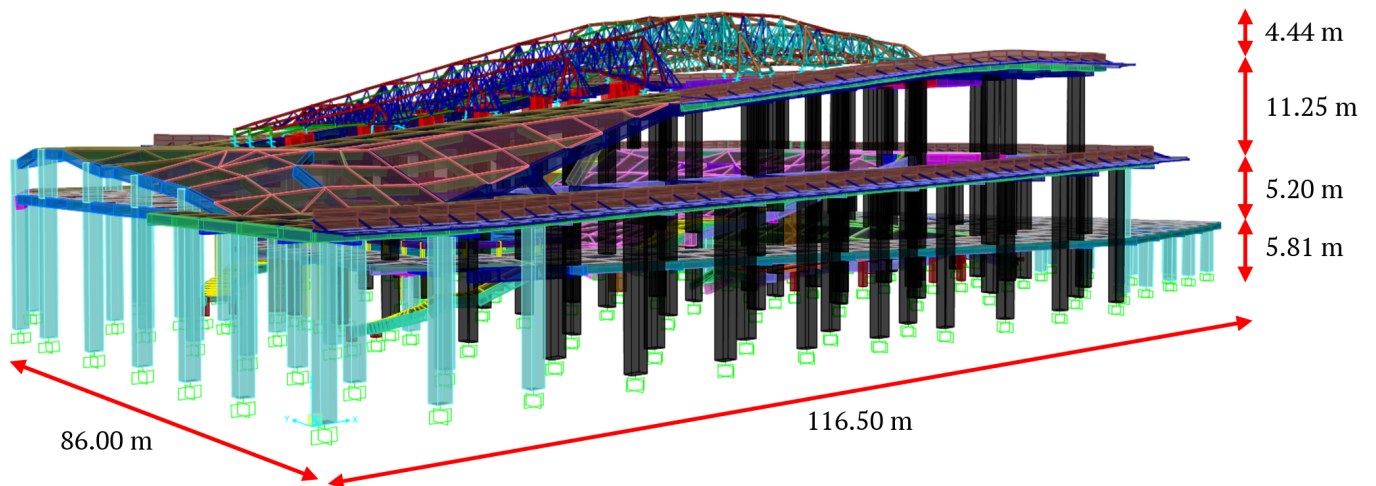


Figure 1 Structural model.

Table 2. Beam cross-sectional data properties.

Type of Beam	Dimension		Longitudinal Reinforcement		Torsion Reinforcement (Middle Side of The Beam)	Confinement Reinforcement
	Width, $B$ (mm)	Depth, $H$ (mm)	Top	Bottom		
B1 End Support	200	350	3 D19	2 D19	-	2 D10-150
B1 Mid Span			2 D19	2 D19	-	2 D10-250
B2 End Support	250	450	6 D19	3 D19	-	2 D10-100
B2 Mid Span			3 D19	3 D19	-	2 D10-200
B3 End Support	250	500	6 D19	3 D19	-	2 D10-150
B3 Mid Span			3 D19	3 D19	-	2 D10-250
B4 End Support	300	600	8 D22	3 D22	-	2 D10-100
B4 Mid Span			3 D22	6 D22	-	2 D10-200
B5 End Support	350	700	10 D22	4 D22	-	2 D13-100
B5 Mid Span			3 D22	8 D22	-	2 D13-200
B6 End Support	400	750	12 D22	5 D22	-	2 D13-100
B6 Mid Span			4 D22	10 D22	-	2 D13-200
B7 End Support	450	850	14 D22	5 D22	-	2 D13-100
B7 Mid Span			5 D22	12 D22	-	2 D13-200
B8 End Support	500	1000	15 D25	6 D25	8 D13	4 D13-150
B8 Mid Span			6 D25	14 D25	8 D13	4 D13-250
B9 End Support	550	1100	15 D25	7 D25	8 D13	4 D13-150
B9 Mid Span			6 D25	15 D25	8 D13	4 D13-250
B10 End Support	600	1200	18 D25	8 D25	10 D13	4 D13-150
B10 Mid Span			8 D25	16 D25	10 D13	4 D13-250
B11 End Support	750	1500	24 D25	10 D25	12 D13	4 D13-200
B11 Mid Span			10 D25	12 D25	12 D13	4 D13-300
B12 End Support	1300	1500	32 D25	16 D25	12 D13	4 D13-200
B12 Mid Span			16 D25	32 D25	12 D13	4 D13-300

ings that require a higher level of confidence in the assessment due to their importance, complexity, or identified risks. The Tier 3 method consisted of 2 analysis procedures, Linear Static Procedure (LSP) and Linear Dynamic Procedure (LDP). Given the building's irregularity, as indicated by previous research, LDP was selected as the more effective approach compared to LSP (Ramdev et al., 2021). The LDP encompasses RSA and LTHA with modal solution type.

For a new building, the selected performance objective, according to ASCE 41-23, is the Basic Performance Objective Equivalent to New Building Standards (BPON). This objective includes two seismic hazard levels: Basic Safety Earthquake 1 and 2 for New Building (BSE-1N and BSE-2N). BSE-1N corresponds to a Design Basis Earthquake (DBE) seismic level, which has a return period of 475 years or a 10% probability of exceedance in 50 years. BSE-2N corresponds to a Maximum Considered Earthquake (MCE) seismic level, which has a return period of 2475 years or a 2% probability of exceedance in 50 years.

Additionally, since the irregular auditorium building is designated as an educational facility, it is categorized as an essential facility and falls under Risk Category IV according to ASCE 7-22 Table 1.5-1. For this risk category, the target performance levels for structural components are: (i) Immediate Occupancy (IO) for BSE-1N, where the building is expected to maintain its pre-earthquake strength and stiffness, ensuring it is safe to occupy; and (ii) Life Safety (LS) for BSE-2N, where the building is expected to maintain safety against partial or total collapse, despite having damaged components.

After performing the analyses, the data obtained from SAP2000, including joint displacements, base reactions, modal information, story forces, and other output items, were further analyzed in Microsoft Excel to check the evaluation results, including modal analysis, building irregularity, and acceptance criteria for each element.

## 2.1 Structural modeling

The irregular Auditorium Building has a total of 3 stories, a Special Moment Frame (SMF) structural system, a truss-shaped steel roof structure, and Stiff Soil (SD) soil type. In addition, the structural components also have large dimensions as mentioned in lines 59-61. The structural data used in this research consisted of material data and cross-section details. The material properties of concrete, rebar, stirrup rebar, and steel profile are displayed in Table 1 while the beam, column, steel pipe, and slab cross-section properties are summarized in Tables 2 to 5. After defining the materials and cross-sectional properties, structural modeling could be conducted by referring to the Detailed Engineering Design

(DED) drawings. The structural model using SAP2000 is presented in Figure 1.

When modeling the structure, the foundation structures were assumed to have fixed supports due to the use of deep foundations, specifically bored piles tied with pile caps with a minimum embedded length of 0.61 m, so that they had rigid properties. For some additional nonstructural components, the foundation structures were assumed to have pinned supports due to the use of shallow foundations, specifically isolated footings, which provided flexible properties.

To adjust for the real condition at the site, where beams and slabs had top-center alignment, the automatic centroid alignment setting in SAP2000 was adjusted to top-center alignment. Additionally, because all the beams were nonprestressed, the reduction factors for flexural and shear rigidity were selected as 0.3 and 0.4, respectively, in accordance with ASCE 41-23. Similarly, for all the columns with design gravity loads less than  $0.1A_g f'_{cE}$  or with tension, the reduction factors for flexural and shear rigidity were also set to 0.3 and 0.4, respectively, in line with ASCE 41-23.

To achieve more accurate results, the slabs were divided into  $1 \times 1 \text{ m}^2$  segments using the meshing tool. This mesh size was chosen according to Rudiyanto (2023), whose mesh evaluation using a convergence study showed that a mesh size of up to 1000 mm produced an error of less than 1%. This mesh size provided the advantage of reducing analysis time without sacrificing accuracy, thus achieving optimal meshing conditions.

All diaphragm elements were assumed to be semi-rigid to better represent the actual structural condition, where most slabs experienced significant out-of-plane deformation, resulting in more flexible behavior. Lastly, the rigid zone factor, or joint stiffness, was set to 0.50 for the reinforced concrete structure, based on the beam-column capacity ratio as stated in ASCE 41-23. An exception was made for the steel roof structure, which had significant shear deformation in the panel zone; for this, the rigid zone factor was set to 0.

## 2.2 Structural loading

The loading calculations were performed for three types of loads: dead load, live load, and seismic load. The roof structure was designed with a curved shape to prevent rainwater from ponding, so the rain load was not considered. Additionally, for low-rise buildings or buildings with spans significantly greater than their height, wind load was ignored, especially in densely populated locations (Mishra and Paliwal, 2019).

When inputting the loads into the structure, ASCE 7-22



Table 3. Column cross-sectional data properties.

Type of Column	Dimension		Longitudinal Reinforcement	Confinement Reinforcement
	Width, $B$ (mm)	Depth, $H$ (mm)		
K1	250	250	9 D16	D8-100 (End Support); D8-200 (Mid-Span)
K2	600	600	20 D22	D10-100 (End Support); D10-200 (Mid-Span)
K3	1000	1000	36 D22	D10-100 (End Support); D10-200 (Mid-Span)
K4	1200	1200	44 D25	D10-100 (End Support); D10-200 (Mid-Span)
K5	1300	800	42 D22	D10-100 (End Support); D10-200 (Mid-Span)
K6	500	1000	22 D22	D10-100 (End Support); D10-200 (Mid-Span)
K7	450	600	20 D22	D10-100 (End Support); D10-200 (Mid-Span)
K8	Diameter, mm: 700		20 D22	D10-100 (End Support); D10-200 (Mid-Span)
KL	300	600	16 D16	D10-100 (End Support); D10-200 (Mid-Span)

Table 4. Steel pipe cross-sectional data properties.

Type of Steel Pipe	Outside Diameter, $D$ (mm)	Wall Thickness, $tw$ (mm)
P4 SCH40	114.30	6.02
P5 SCH40	141.30	6.55
P6 SCH40	168.30	3.40
P8 SCH40	219.1	8.18
P10 SCH40	273.10	15.10

guidelines were followed. The effective seismic weight included 100% of the dead load, which consisted of both the self-weight load and any additional dead loads, and 25% of the live load. According to ASCE 41-23, for linear analysis procedures, a damping ratio of 5% was used for all seismic loads. Additionally, P- $\Delta$  effects were considered and automatically applied to the building by assigning them to the modal load in the load case section.

Seismic load consisted of response spectrum load and time history load. For the response spectrum load, the spectral response acceleration parameters were retrieved from the Indonesia Earthquake Hazard Deaggression Map for Earthquake-Resistant Infrastructure Planning and Evaluation 2022, focusing on the Yogyakarta area. These parameters included: (i) Short period (0.2 seconds,  $S_s$ ) with a value of 1.00 g; and a long period (1.0 seconds,  $S_1$ ) with a value of 0.45 g. These values corresponded to the Maximum Considered Earthquake (MCE) seismic hazard levels, with a return period of 2475 years or a 2% probability of exceedance in 50 years, and a 5% damping ratio. Using these values, the horizontal (Figure 2a) and vertical response spectrum (Figure 2b) target graphs were generated according to ASCE 7-22.

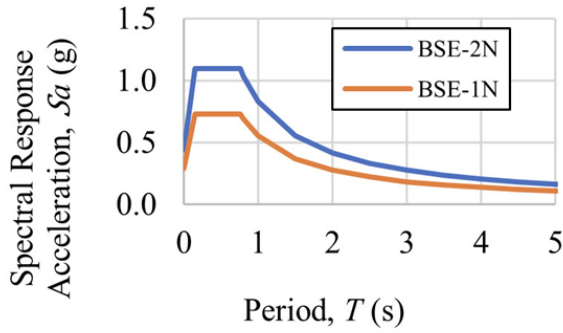
Meanwhile, for the time history load, the selection of ground motion data was based on Indonesia

Table 5. Slab cross-sectional data properties.

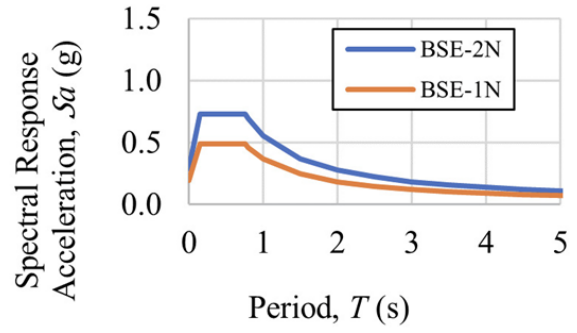
Type of Slab	Thickness, $t$ (mm)	Reinforcement
130 mm Slab - Indoor	130	D10-100 (2 layers)
130 mm Slab - Outdoor	130	D10-100 (2 layers)
130 mm Slab - Stage	130	D10-100 (2 layers)
180 mm Slab - Outdoor	180	D10-100 (2 layers)
130 mm Slab - Ramp	130	D10-100 (2 layers)
150 mm Slab - Ramp	150	D10-100 (2 layers)
Staircase Slab	120	D10-100 (2 layers)
Upper Tribune Slab	120	D10-100 (2 layers)
Lower Tribune Slab	120	D10-100 (2 layers)

Earthquake Hazard Deaggression Map for Earthquake-Resistant Infrastructure Planning and Evaluation 2022 with a minimum of 3 ground motion pairs for the linear analysis procedure according to ASCE 7-22. All ground motion data were selected considering the values of magnitude, range, and velocity to find the most suitable ground motions to represent earthquakes in Indonesia. The selected ground motion pairs are shown in Table 6 and Appendices.

As stated in ASCE 41-23, each ground motion must be matched spectrally with the period range of  $0.8 \times T_{lower}$  to  $1.2 \times T_{upper}$  where  $T_{lower}$  was retrieved from the building's period from modal analysis where 90% of the mass of the building has been obtained in every direction, and  $T_{upper}$  was retrieved from the largest value of the building's period from modal analysis in orthogonal direction. The results of spectral matching of average pseudo-acceleration of three pairs of ground motions with seismic hazard levels BSE-1N and BSE-2N is shown in Figure 3 and the graph of relative percentage of average spectral matching of ground motion accelerations is shown in Figure 4. With the  $T_{lower}$  of 0.11 seconds and the  $T_{upper}$  of 0.71 seconds, the average relative ground motion recordings which were matched in the range of  $0.8 T_{lower}$  at 0.09 seconds and  $1.2 T_{upper}$  at 0.85 seconds were in compliance with the +10% limit of the target spectrum.



(a) Horizontal direction



(b) Vertical direction

Figure 2 Spectrum response graph in: (a) horizontal direction, and (b) vertical direction.

Table 6. The selected ground motion data.

Mechanism of Earthquakes	Earthquake Name and Location	Year	Station	Magnitude, $M(M_w)$	Range of Rupture, $R_{rup}$ Km	Velocity, $V_{s30}$ ( $m_s$ )
Shallow Crustal	Victoria, Mexico	1980	Chihuahua	6.33	20.96	242.05
Megathrust	South America	2010	Vina Del Mar Centro (Galeria Couve)	8.81	119.52	282.00
Benioff	Iwate Off, Japan	2011	Hanamaki-S	7.40	119.02	288.80

For the load combination, basically, there are 2 types of loads based on the duration of loading, namely permanent load and temporary load. Load combination must be formulated so that the capacity of each structural element can withstand all possible combinations of factorized loads. To define the load combination, it is necessary to follow several requirements described in ASCE 41-23 as follows:

1. Gravity load combination For linear procedures, if the effects of gravity loads and seismic forces are additive, then the combination of gravity loads should be obtained from Equation (1). Whereas, if the effects of gravity loads and seismic forces are counteracting, then the combination of gravity loads should be obtained from Equation (2).

$$Q_G = 1.1 \times (Q_D + Q_L) = 1.1(Q_D + 0.25Q_L) = 1.1Q_D + 0.275Q_L \quad (1)$$

$$Q_G = 0.9 \times Q_D \quad (2)$$

2. Deformation-Controlled Actions (DCA) combination For linear procedures, combination of DCA must be calculated based on Equation (3).

$$Q_{UD} = Q_G + Q_E \quad (3)$$

where  $Q_{UD}$  is combination of DCA and  $Q_E$  is seismic

Table 7. Alternative value of  $C_1 C_2$  (ASCE 41-23, 2023).

Fundamental Period (T)	$m_{max} < 2$	$2 \leq m_{max} < 6$	$m_{max} \geq 6$
T is lower than 0.5	1.1	1.4	1.8
T is lower than 1.0 but higher than 0.3	1.0	1.1	1.2
T is higher than 1.0	1.0	1.0	1.1

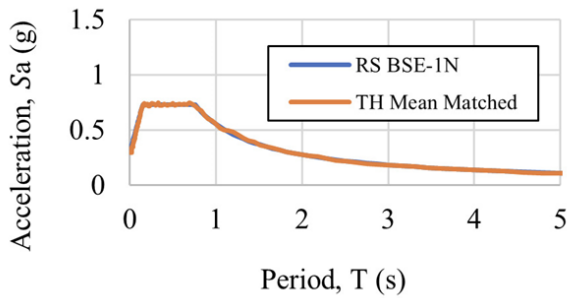
loads (either response spectrum loads or time history loads).

3. Force-Controlled Actions (FCA) combination For linear procedures, combination of FCA must be calculated based on Equation (4).

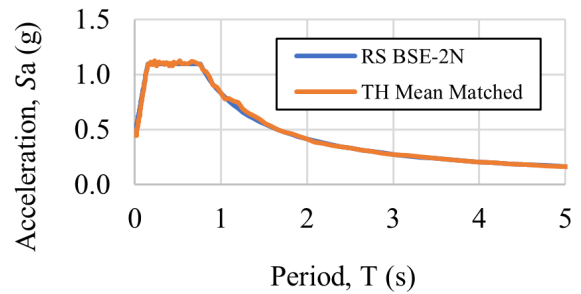
$$Q_{UF} = Q_G + \frac{\chi Q_E}{C_1 C_2 J} \quad (4)$$

where  $Q_{UF}$  is combination of FCA,  $\chi$  is factor to adjust an action generated by response of the building for the selected performance level (1.3 for Life Safety or Immediate Occupancy), J is force-delivery reduction factor for certain level of seismicity (2.0 for structure with high seismicity level but as an exception, 1.0 shall be taken if the chosen structural performance level is Immediate Occupancy), and  $C_1 C_2$  can be obtained from Table 7.

where T is fundamental period of a reviewed building in a certain direction (s), obtained from modal analysis, and  $m_{max}$  is the highest m-factor for all primary components of the building under review in a certain direction.

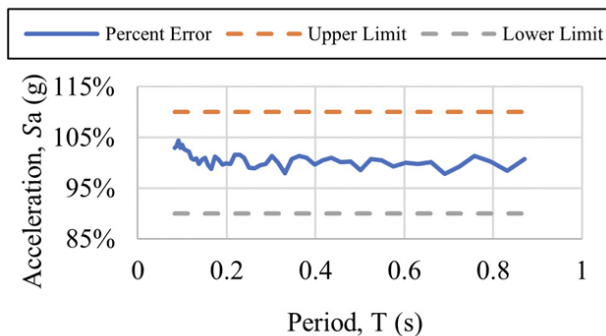


(a) BSE-1N

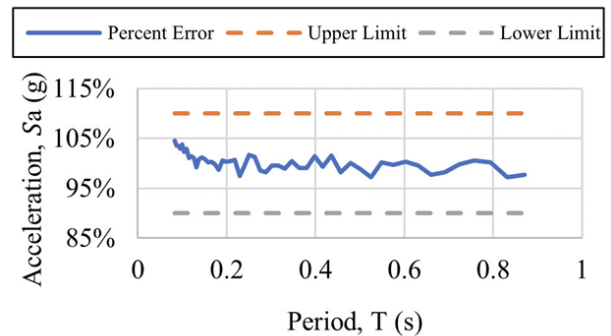


(b) BSE-2N

Figure 3 Spectral matching results between average pseudo-acceleration and response spectrum for: (a) BSE-1N, and (b) BSE-2N.



(a) BSE-1N



(b) BSE-2N

Figure 4 Relative percent error of average matched ground motion recordings for: (a) BSE-1N, and (b) BSE-2N.

### 2.3 Modal Analysis

Modal analysis should be carried out first to identify the behavior of the building under review by checking the modal shape and the combined modal mass participation of the building. Modal shape can be seen from the dominant mass participation between the x-direction, y-direction, and z-direction. In addition, according to ASCE 41-23, the total combined modal mass participation must reach at least 90% of the actual mass of the structure in each orthogonal direction.

### 2.4 Building Irregularity Check

Irregularity checks were conducted using two different methods: the response spectrum method and the time history method. Types of building irregularity are listed as follows:

1. In-plane discontinuity irregularity: This is assumed to be present in any primary component of a seismic-force-resisting system if a component exists at one floor, but it is offset in the plane of the component at the adjacent floor.
2. Out-of-plane discontinuity irregularity: This is assumed to be present in any primary component of a

seismic-force-resisting system if a component exists at one floor, but it is offset out of the plane to the component in an adjacent floor.

3. Weak story irregularity: This is assumed to be present in any direction of the building if the average Demand-Capacity Ratio (DCR) in any floor to the adjacent floor in the same direction is more than 125%.
4. Torsional strength irregularity: This is assumed to be present in any direction of the building if the diaphragm above the floor under review is inflexible and, in the same direction, the critical action DCR ratio of primary components on one side of the floor center of resistance to the critical action DCR of primary components on the other side of the floor center of resistance is more than 1.5.

### 2.5 Linear analysis procedure

Linear analysis procedures can be performed for buildings that do not have any irregularities. Based on ASCE 41-23, if a building has one or more of those irregularities, then linear procedures cannot be used for the building unless the DCR of all components in the building is smaller than the minimum value between 3.0 and the m-factor of each component. The magnitude of

DCR can be calculated using Equation (5).

$$DCR = \frac{Q_{UD}}{Q_{CE}} \quad (5)$$

where  $Q_{CE}$  is the expected strength of the component.

## 2.6 Acceptance criteria

Before determining the acceptance criteria for the components, each action on the components must be labeled as either deformation-controlled (ductile) or force-controlled (brittle). A ductile component tends to fail due to the deflection that occurs in the component, so it needs to be controlled for its deformation. In contrast, a brittle component tends to experience a sudden failure due to the load applied to the component, so that it needs to be controlled for its force. To determine which type of forces must be categorized as ductile or brittle, ASCE 41-23 and ACI 318-19 can be used as guidelines. Therefore, in accordance with those building codes, evaluation procedures are divided into 4 categories: DCA evaluation for beam moment, FCA evaluation for beam shear, DCA evaluation for column axial force and biaxial moment (PMM), and FCA evaluation for column shear.

The acceptance criteria for DCA of a new building can be calculated with the Equation (6):

$$mQ_{CE} > Q_{UD} \quad (6)$$

where  $m$  is the modification factor, used to account for the expected ductility of the elements and whose value varies depending on the elements, and  $\phi$  is the knowledge factor, used to account uncertainty in the collection of as-built data whose value is 1 in this research.

On the other hand, the acceptance criteria for Force-Controlled Action (FCA) of a new building can be calculated with the Equation (7):

$$Q_{CL} > Q_{UF} \quad (7)$$

where  $Q_{CL}$  is the lower-bound strength of the component.

## 3 RESULTS

### 3.1 Modal analysis result

Table 8. Modal shape based on the dominant mass participation.

Modal Shape	Period, $T$ (s)	X-Direction	Y-Direction	Z-Direction
1	0.71	4.03%	47.86%	18.74%
2	0.68	10.92%	13.79%	38.02%
3	0.62	50.22%	0.06%	15.32%

Table 9. Combined modal mass participation.

Modal Shape	Period, $T$ (s)	Sum in X-Direction	Sum in Y-Direction	Sum in Z-Direction
250	0.11	90.48%	92.57%	97.01%

### 3.1.1 Modal shape

The modal shape analysis results provide important insights into the dynamic behavior of the structure. For the first modal shape, the dominant mass participation is in the Y-direction, accounting for 47.86%, suggesting potential flexibility or vulnerability in this direction, while the X-direction is minimal at 4.03%. In the second modal shape, the primary response shifts to the Z-direction with a mass participation of 38.02%. The Y-direction participation is moderate at 13.79%, and the X-direction is at 10.92%. The third modal shape reveals a dominant response in the X-direction, with mass participation of 50.22%, highlighting the building's primary movement along the X-axis, while the Y-direction is almost negligible at 0.06% (Table 8). The first three modal shapes of the building, as considered from the shape of the building movement due to modal load, are displayed in Figure 5. From these data, it can be seen that the first three modal shapes were translation in the Y-direction, rotation in the Z-direction, and translation the X-direction.

### 3.1.2 Combined modal mass participation

The total mass participation results obtained from the modal analysis are shown in Table 9. These results reveal that to achieve at least 90% mass participation of the building, as required in Section 2.3, a total of 250 modes are necessary. Specifically, the sum of mass participation in the X-direction is 90.48%, in the Y-direction is 92.57%, and in the Z-direction is 97.01%. Capturing at least 90% of the mass participation in modal analysis is essential to ensure an accurate and comprehensive representation of the building's dynamic behavior.

### 3.2 Building irregularity and Demand-Capacity Ratio (DCR) check

The building satisfies the requirements for in-plane discontinuity, out-of-plane discontinuity, and weak



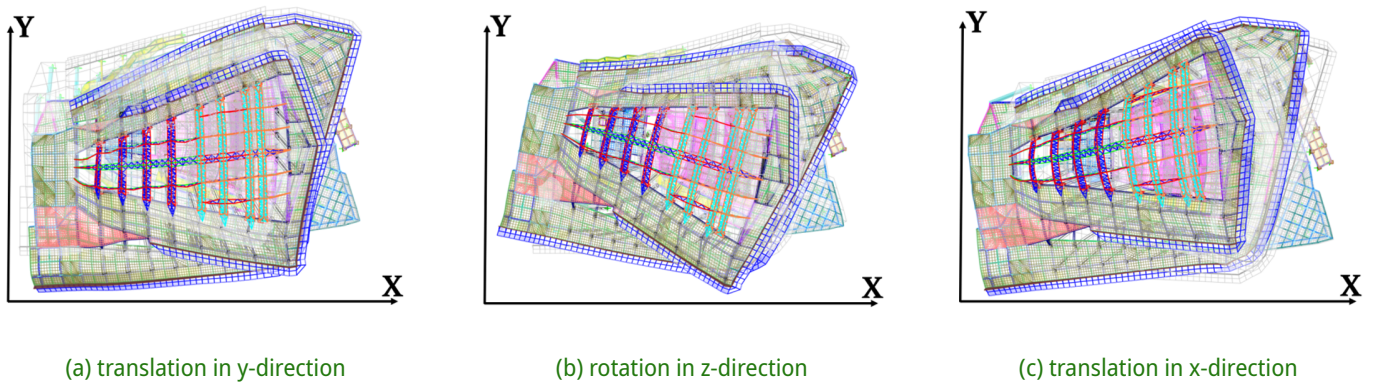


Figure 5 Modal shape based on building movement due to modal load: (a) translation in y-direction, (b) rotation in z-direction, and (c) translation in x-direction.

Table 10. Summary of building irregularity.

Seismic Hazard Level	Method	Building Irregularity			
		In-Plane Discontinuity	Out-of-Plane Discontinuity	Weak Story	Torsional Strength
BSE-1N	RS	Did not exist	Did not exist	Did not exist (Max: 116.50%)	Existed (Max: 3.78)
	TH	Did not exist	Did not exist	Did not exist (Max: 109.75%)	Existed (Max: 3.61)
BSE-2N	RS	Did not exist	Did not exist	Did not exist (Max: 114.79%)	Existed (Max: 3.79)
	TH	Did not exist	Did not exist	Did not exist (Max: 110.15%)	Existed (Max: 3.18)

story irregularities as shown in Table 10. However, it does not meet the requirements for torsional strength irregularity, as outlined in Section 2.4, indicating that the building has torsional strength irregularity. Consequently, if a linear analysis procedure is used, it is necessary to verify the DCR values as specified in Section 2.5. Table 11 reveals that 9.87% of the total components exceeded the maximum DCR limit according to the FCA evaluation using the LTHA method. Specifically, out of 1661 components, 5.42% of beams and 8.49% of columns exceeded the limit in response spectrum (RS) analysis, while 7.65% of beams and 9.87% of columns exceeded the limit in time history (TH) analysis.

### 3.3 Evaluation result

#### 3.3.1 DCA evaluation of beam moment

The evaluation results of beam moment using both RSA and LTHA methods are shown in Table 12 and Figure 6. From these data, it can be seen that in the DCA evaluation of beam moment using RSA method, the highest ratio of the maximum value was 1.831 for BSE-1N and 2.290 for BSE-2N while the highest ratio of the mean value was 0.229 for BSE-1N and 0.205 for BSE-2N. In contrast, using LTHA method, the highest ratio of the maximum value was 2.198 for BSE-1N and 3.071 for BSE-2N while the highest ratio of the mean value was 0.294 for BSE-1N and 0.259 for BSE-2N.

Table 11. Total number of components with DCR value greater than the maximum limit.

Component Type	Total Components	DCA		FCA	
		RS	TH	RS	TH
Beam	1300	20	28	49	80
Column	361	70	113	78	84
Total	1661	90	141	127	164
Percentage		5.42%	8.49%	7.65%	9.87%

#### 3.3.2 FCA evaluation of beam shear

The evaluation results of beam shear using both RSA and LTHA methods are shown in Table 13 and Figure 7. From these data, it can be observed that in FCA evaluation of beam shear using RSA method, the highest ratio of the maximum value was 3.441 for BSE-1N and 2.332 for BSE-2N, while the highest ratio of the mean value was 0.548 for BSE-1N and 0.416 for BSE-2N. In contrast, using LTHA method, the highest ratio of the maximum value was 3.662 for BSE-1N and 2.817 for BSE-2N, while the highest ratio of the mean value was 0.688 for BSE-1N and 0.478 for BSE-2N.

#### 3.3.3 DCA evaluation of column axial force and biaxial moment (PMM)

The evaluation results of column PMM using both RSA and LTHA methods are shown in Table 14 and Figure 8. From these data, it can be observed that in DCA

Table 12. DCA evaluation of beam moment.

Story	$Q_{UD}/mQ_{CE}$							
	RSA Method				LTHA Method			
	Max (IO)	Mean (IO)	Max (LS)	Mean (LS)	Max (IO)	Mean (IO)	Max (LS)	Mean (LS)
1	0.981	0.167	1.143	0.146	1.338	0.215	1.357	0.185
2	1.831	0.229	2.290	0.205	2.198	0.294	3.071	0.259
3	0.605	0.117	0.736	0.114	0.819	0.156	0.901	0.146

Table 13. FCA evaluation of beam shear.

Story	$Q_{UF}/Q_{CL}$							
	RSA Method				LTHA Method			
	Max (IO)	Mean (IO)	Max (LS)	Mean (LS)	Max (IO)	Mean (IO)	Max (LS)	Mean (LS)
1	2.269	0.421	1.583	0.321	2.782	0.539	1.651	0.379
2	3.441	0.548	2.332	0.416	3.662	0.688	2.817	0.478
3	1.777	0.336	1.239	0.256	2.263	0.428	1.366	0.302

evaluation of column axial force and biaxial moment (PMM) using RSA method, the highest ratio of the maximum value was 2.089 for BSE-1N and 3.117 for BSE-2N, while the highest ratio of the mean value was 0.765 for BSE-1N and 0.719 for BSE-2N. In contrast, using LTHA method, the highest ratio of the maximum value was 2.843 for BSE-1N and 4.156 for BSE-2N, while the highest ratio of the mean value was 0.934 for BSE-1N and 0.812 for BSE-2N.

### 3.3.4 FCA evaluation of column shear

The evaluation results of column shear using both RSA and LTHA methods are shown in Table 15 and Figure 9. From these data, it can be known that in FCA evaluation of column shear using RSA method, the highest ratio of the maximum value was 3.375 for BSE-1N and 2.725 for BSE-2N, while the highest ratio of the mean value was 0.689 for BSE-1N and 0.490 for BSE-2N. Whereas, using LTHA method, the highest ratio of the maximum value was 5.595 for BSE-1N and 4.396 for BSE-2N, while the highest ratio of the mean value was 0.898 for BSE-1N and 0.587 for BSE-2N.

### 3.3.5 Components with acceptance criteria ratio greater than 1

The results for the BSE-1N (Immediate Occupancy) and BSE-2N (Life Safety) seismic hazard levels across different stories and analysis methods reveal varying levels of exceedance of acceptance criteria ratios greater than 1 (Table 16). For the DCA evaluation, the exceedance percentages ranged from 4.76% to 11.74% for BSE-1N and 5.60% to 21.85% for BSE-2N. In con-

trast, the FCA evaluation showed a more pronounced exceedance, particularly in the BSE-2N scenario, with values ranging from 11.74% to 21.85%. Notably, the highest exceedance of 21.85% occurred in the FCA evaluation for BSE-2N using the RSA method.

### 3.3.6 Summary of the performance level of each component

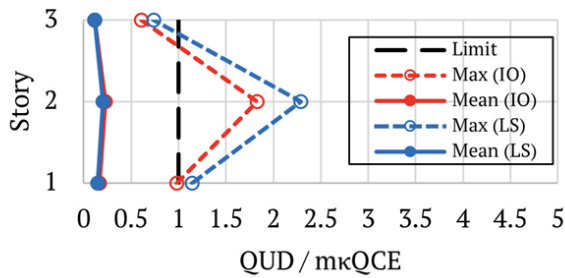
The summary of the evaluation results as explained in Section 3.3.1 to Section 3.3.4 is displayed in Table 17. From the data, it can generally be observed that with the mean value, all target performance levels have been achieved while with the maximum value, all target performance levels have not yet been fully met.

The data indicates that, on average, all target performance levels were achieved. For the BSE-1N seismic hazard level, both beams and columns met the Immediate Occupancy (IO) performance level across all analysis methods (DCA and FCA) and for both Response Spectrum (RS) and Time History (TH) analyses. Similarly, for the BSE-2N seismic hazard level, all components achieved the Life Safety (LS) performance level on average.

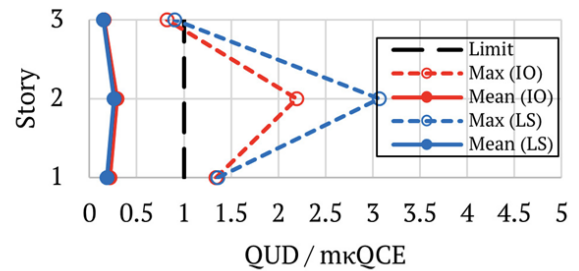
However, when considering the maximum values, none of the target performance levels were fully met. For both seismic hazard levels, the performance levels exceeded the IO and LS targets, respectively, indicating that the maximum demands on the components were higher than the specified performance criteria. This discrepancy suggests that while the structure generally meets the performance objectives under typical conditions, there are instances where the performance re-

Table 14. DCA evaluation of column axial force and biaxial moment.

Story	$Q_{UD}/mQ_{CE}$							
	RSA Method				LTHA Method			
	Max (IO)	Mean (IO)	Max (LS)	Mean (LS)	Max (IO)	Mean (IO)	Max (LS)	Mean (LS)
1	2.089	0.522	3.117	0.571	2.843	0.681	4.156	0.719
2	1.362	0.765	1.472	0.719	1.768	0.934	1.953	0.812
3	1.779	0.683	2.648	0.657	2.100	0.894	3.128	0.780



(a) using RSA method



(b) using LTHA method

Figure 6 DCA evaluation of beam moment: (a) using RSA method, and (b) using LTHA method.

quirements are not fully satisfied under maximum load scenarios.

#### 4 DISCUSSIONS

##### 4.1 Modal analysis result

##### 4.1.1 Modal shape

The analysis results from Table 8 and Figure 5 reveal discrepancies between the building’s expected response and the actual modal shapes observed. The first three modal shapes indicate primary movements of the building that do not align with typical expectations for structural behavior. Specifically, it is anticipated that the first and second modal shapes would involve translation, while the third modal shape involves rotation (Kada and Sharma, 2022). However, we found that the first modal shape shows a predominant translation in the Y-direction, the second modal shape involves ro-

Table 16. Percentage of all components with acceptance criteria ratio greater than 1.

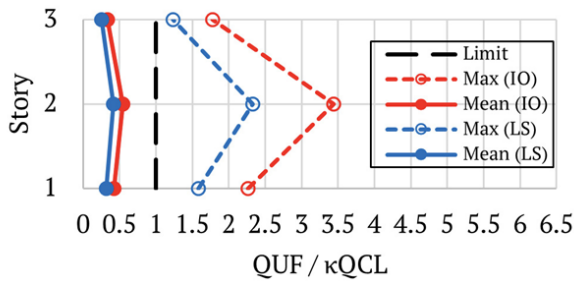
Story	DCA				FCA			
	BSE-1N (IO)		BSE-2N (LS)		BSE-1N (IO)		BSE-2N (LS)	
	RS	TH	RS	TH	RS	TH	RS	TH
1	2.29%	3.21%	5.20%	5.05%	8.72%	2.75%	17.43%	5.66%
2	8.69%	9.57%	12.08%	11.49%	18.11%	5.15%	30.34%	10.01%
3	1.52%	2.13%	5.79%	3.96%	4.57%	1.52%	13.11%	3.35%
Total	4.76%	5.60%	8.13%	7.47%	11.74%	3.49%	21.85%	6.98%

Table 17. Summary of the performance level of each component.

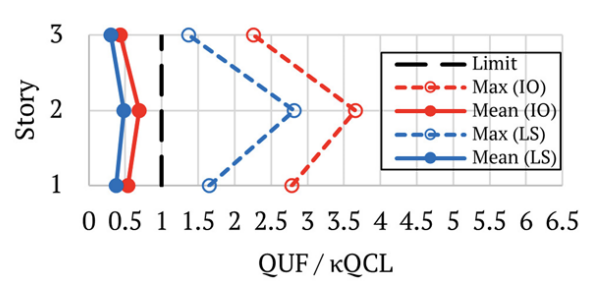
Seismic Hazard Level	Value	Beam				Column			
		DCA		FCA		DCA		FCA	
		RS	TH	RS	TH	RS	TH	RS	TH
BSE-1N	Mean	IO	IO	IO	IO	IO	IO	IO	IO
	Max	>IO	>IO	>IO	>IO	>IO	>IO	>IO	>IO
BSE-2N	Mean	LS	LS	LS	LS	LS	LS	LS	LS
	Max	>LS	>LS	>LS	>LS	>LS	>LS	>LS	>LS

Table 15. FCA evaluation of column shear.

Story	$Q_{UF}/Q_{CL}$							
	RSA Method				LTHA Method			
	Max (IO)	Mean (IO)	Max (LS)	Mean (LS)	Max (IO)	Mean (IO)	Max (LS)	Mean (LS)
1	3.375	0.486	2.725	0.347	5.595	0.675	4.396	0.460
2	2.182	0.689	1.745	0.490	2.814	0.898	1.744	0.587
3	2.808	0.567	2.156	0.401	3.883	0.779	3.150	0.515

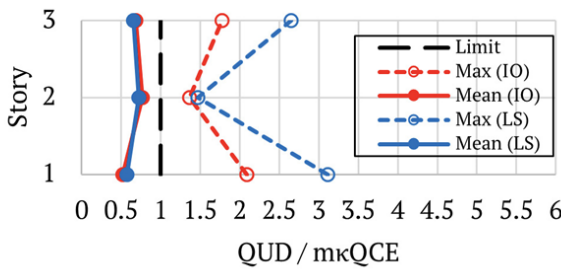


(a) using RSA method

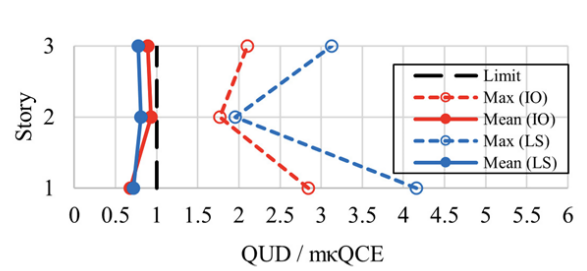


(b) using LTHA method

Figure 7 FCA evaluation of beam shear: (a) using RSA method, and (b) using LTHA method.



(a) using RSA method



(b) using LTHA method

Figure 8 DCA evaluation of column axial force and biaxial moment (PMM): (a) using RSA method, and (b) using LTHA method.

tation in the Z-direction, and the third modal shape is characterized by translation in the X-direction. The presence of significant rotation in the Z-direction in the second modal shape is noteworthy. This rotation could be attributed to the building’s irregular shape, which affects its dynamic behavior and load distribution (Jyothi and Sekhar, 2022). In regular buildings, modal shapes often reflect more straightforward patterns of movement, but in this case, the irregularity introduces complex rotational effects (Lee et al., 2016).

Given these findings, it is crucial to perform further analysis using the evaluation procedures outlined in ASCE 41-23. This additional analysis will help assess the building’s performance under these complex modal behaviors and ensure that the design addresses potential vulnerabilities introduced by the building’s irregular shape. Specifically, the rotation observed in the second modal shape could impact the building’s torsional response and overall stability, necessitating a thorough evaluation to confirm that the structure meets safety and performance criteria under dynamic loading conditions.

#### 4.1.2 Combined modal mass participation

In seismic analysis, when the response spectrum analysis method is applied, the accuracy of this approach relies on the proportion of the total building mass included in the modal analysis, known as the mass participation ratio (MPR). Most building codes require a

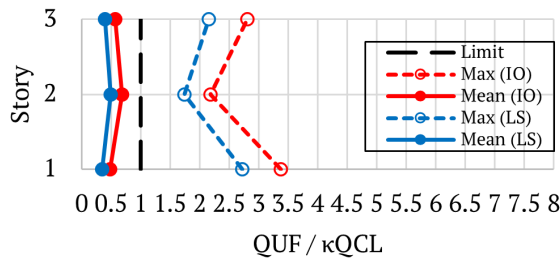
minimum MPR of 90% and to achieve that, a sufficient number of mode shapes (NOMS) must be included. Generally, it is expected that buildings require approximately 12 modes to reach 90% mass participation in each direction (Caldi et al., 2020).

In the case of buildings with irregularities and complex structures, achieving the 90% MPR requires a very large NOMS. This can be explained by the fact that in regular buildings, structural components participate in modes with longer period whereas in irregular buildings, they do not. In order for all structural components in an irregular building to participate, modes with very short periods should be recalled which sometimes is hard to achieve (Hanna et al., 2017). The greater the number of modes required, the more the dynamic response of the structure is accommodated, but the longer the analysis takes. In this study, to reach the 90% MPR, the analysis needed to include a certain number of modes, which from Table 9, shows that the number of modes needed was 250.

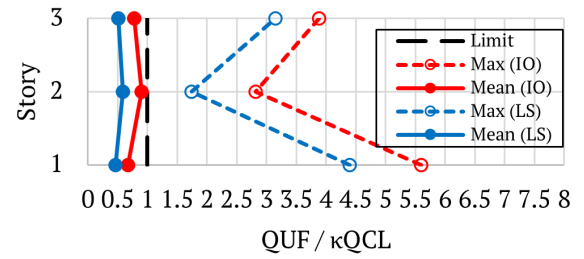
#### 4.2 Building irregularity and Demand-Capacity Ratio (DCR) check

Irregular auditorium building did not have in-plane discontinuity irregularity and out-of-plane discontinuity irregularity because there was no primary element at one level that did not continue or was offset either within the plane of the element or out of the plane of the element at the adjacent level. Then, to determine





(a) using RSA method



(b) using LTHA method

Figure 9 FCA evaluation of column shear: (a) using RSA method, and (b) using LTHA method.

whether the weak story irregularity exists or not, the average DCR in one story must be calculated and compared to the adjacent story, both the story above and the story below. After calculating the average DCR, it could be found that this irregularity did not exist because the maximum percentage was 116.50%, which was less than 125%. Lastly, to find out whether the torsional strength irregularity exists or not, the DCR ratio on one side of story must be calculated and compared to the other side of the story. After calculating the DCR ratio on each side of the story, it could be found that this irregularity existed because the maximum ratio was 3.79, which was more than 1.5.

Because the building had a torsional irregularity, the linear procedure is permitted to be applied to the building if only the DCR of all components in the building is less than the smallest between 3.0 and the m-factor of each component. From the Table 11, there were still many components that had DCR values greater than the maximum limit, but since the largest percentage of the components that did not meet the requirements was only 9.87% of the total components, the linear procedure was assumed to be applicable.

### 4.3 Evaluation result

From Tables 12 to 15 and Figures 6 to 9, it can be seen that the mean values, using both RSA and LTHA methods, in both BSE-1N and BSE-2N seismic hazard levels, were less than 1, indicating that all structural components had met the requirements of the acceptance criteria. However, the maximum values still exceeded 1, showing that some of the components still did not meet the requirements of the acceptance criteria. Therefore, it can be concluded that in BSE-1N seismic hazard level, the average performance of all structural components was Immediate Occupancy (IO) and the maximum performance of all structural components did not meet the Immediate Occupancy performance level target while in BSE-2N seismic hazard level, the average performance of all structural components was Life Safety (LS) and the maximum performance of all structural components did not meet the Life Safety performance level

target. In addition, from the data in Table 16, it can be found the largest percentage of all components with ratio value greater than 1 was 21.85%, which occurred in the FCA evaluation in BSE-2N seismic hazard level using RSA method.

Moreover, from the summary in Table 17, it can be concluded that with the mean value of the acceptance criteria ratio in BSE-1N seismic hazard level, the Immediate Occupancy performance level had been complied for all beams and columns in every evaluation procedure and every analysis method. Meanwhile, with the mean value of the acceptance criteria ratio in BSE-2N seismic hazard level, the Life Safety performance level had been complied for all beams and columns in every evaluation procedure and every analysis method. On the contrary, with the maximum values of the acceptance criteria ratio in BSE-1N seismic hazard level, all beams and columns in every evaluation procedure and every analysis method did not meet the Immediate Occupancy performance level target. Whereas, with the maximum values of the acceptance criteria ratio in BSE-2N seismic hazard level, all beams and columns in every evaluation procedure and every analysis method did not meet the Life Safety performance level target.

According to the results, some of the structural components still did not meet the performance level target. It might occur due to the different criteria of seismic analysis from the design stage. For irregular building, if the elastic design is used, then the ductility of every component is assumed to be uniform while it actually depends on the rebar configuration of each element. Besides that, the response of each structural element is variable where deformation can occur at certain points of the building. This condition is called the plastic state of a structure. Plastic state is defined as a state where the element deforms irreversibly and does not return to its initial shape and dimension, even if the load is already removed. Plastic state can only be observed with nonlinear analysis procedures because of the nonlinear behavior of the structures. For that reason, nonlinear evaluation procedures should be conducted in order to take into account any behaviors that may affect the structure, such as large deformations, plasticity, crack-

ing, or other nonlinear behavior. In addition, nonstructural components, such as stairs, masonry walls, partition walls, and similar components, and lower structural components, including tie beams, ground floor slabs, and foundation structures can also be modeled and evaluated.

#### 4.4 Comparison between RSA Method and LTHA Method

From Tables 12 to 15 and Figures 6 to 9, it can be seen that LTHA method produced a higher acceptance criteria ratio than RSA method. Meanwhile, from Table 16, it can be seen that RSA method gave a higher number of components with acceptance criteria ratio exceeding 1 than LTHA method. The results differed from the previous studies, as in Ramdev, et al (2021), Zagade, et al (2021), Suryanto (2018), and Chandrakar, et al (2017), who stated that the RSA method would overestimate the stresses while LTHA method would give a more precise approximation. Therefore, the results obtained using RSA method should typically be higher than using LTHA method. These differences could occur due to the application of the concurrent seismic effects in this study, where in this research, the RSA method was applied using a combination of 100% and 30%, while LTHA method was applied using a combination of 100% and 100%.

## 5 CONCLUSION

From both RSA and LTHA methods, it can be concluded that the average performance level of all beams and columns in BSE-1N seismic hazard level, for DCA and FCA evaluations, was Immediate Occupancy (IO), where the result met the expected performance level target. However, the maximum performance level of all beams and columns in BSE-1N seismic hazard level, for both DCA and FCA evaluations, did not meet the IO performance level target. Meanwhile, the average performance level of all beams and columns in BSE-2N seismic hazard level, for both DCA and FCA evaluations, was Life Safety (LS), where the result met the expected performance level target. However, the maximum performance level of all beams and columns in BSE-2N seismic hazard level, for both DCA and FCA evaluations, did not meet the LS performance level target. Some structural components that did not comply with the performance level target were caused by linear assumption with response spectrum analysis in the structural design. Therefore, when designing an irregular building structure, it is recommended to evaluate the seismic performance by referring to ASCE 41-23 as a recheck to verify the safety of the design. Furthermore, for future research, nonlinear evaluation procedures should be performed in order to obtain more accurate and more reliable results, and nonstructural components should also be considered and evaluated.

## DISCLAIMER

The authors declare no conflict of interest.

## ACKNOWLEDGMENTS

The authors are grateful for the facilities provided by the Computer Laboratory in Department of Civil and Environmental Engineering, Gadjah Mada University.

## REFERENCES

- Alecci, V. and Stefano, M. D. (2019), 'Building irregularity issues and architectural design in seismic areas', *Frattura ed Integrità Strutturale*.  
**URL:** <https://doi.org/10.3221/IGF-ESIS.47.13>
- ASCE (2023), *ASCE 41-23 Seismic Evaluation and Retrofit of Existing Buildings*, American Society of Civil Engineers, Reston, Virginia.
- Aysha, S. (2021), 'A comparative study on seismic performance evaluation between reinforced concrete structures and post tensioned concrete structures using etabs', *International Journal of Latest Engineering Research and Applications (IJLERA)*.
- Caldi, F. et al. (2020), Evaluating the modal response of linked tall buildings, Council on Tall Buildings and Urban Habitat (CTBUH), Chicago, USA.
- Chandrakar, P. and Bokare, P. S. (2017), 'A review – comparison between response spectrum method and time history method for dynamic analysis of multistoried building', *RSR Rungta College of Engineering and Technology*.
- Hanna, N. F. et al. (2017), 'Efficient mass participation ratio of building with basement', *IOSR Journal of Mechanical and Civil Engineering*.  
**URL:** <https://doi.org/10.9790/1684-1401045974>
- Hussein, G., Eid, N. and Khaled, H. (2019), 'Torsional behavior of irregular structures during earthquakes', *IOSR Journal of Mechanical and Civil Engineering*.  
**URL:** <https://doi.org/10.9790/1684-1605044055>
- Jyothi, S. and Sekhar, R. (2022), 'Design and analysis of irregular shape building in staad pro', *Journal of Engineering Sciences*.
- Kada, H. A. and Sharma, R. R. (2022), 'Parametric study of factors influencing mode shape of oscillation', *International Journal of Engineering Research and Applications (IJERA)*.
- Lee, X. S., Yan, C. P. and See, Z. S. (2016), Irregular shaped building design optimization with building information modelling, in 'MATEC Web of Conferences', Vol. 66, Kuala Lumpur, Malaysia.  
**URL:** <https://doi.org/10.1051/mateconf/20166600027>

Manoj, J. S. and Varghese, R. G. (2022), 'Analysis of irregular building using response spectrum method in etabs', *International Journal of Engineering Research & Technology (IJERT)*.

Mishra, S. N. and Paliwal, M. C. (2019), 'Wind load analysis for different configuration of structures', *International Research Journal of Engineering and Technology (IRJET)*.

Nady, O., Mahfouz, S. Y. and Taher, S. E.-D. F. (2022), 'Quantification of vertical irregularities for earthquake resistant reinforced concrete buildings', *MDPI (Multidisciplinary Digital Publishing Institute)*.

**URL:** <https://doi.org/10.3390/buildings12081160>

Nurwihastuti, D. W. et al. (2014), 'Understanding of earthquake damage pattern through geomorphological approach: A case study of 2006 earthquake in bantul,

yogyakarta, indonesia', *World Journal of Engineering and Technology*.

**URL:** <https://doi.org/10.4236/wjet.2014.23B010>

Paul, A., Parvez, Z. and Morshed, A. Z. (2023), Study on seismic responses of plan irregular buildings due to torsional irregularity and re-entrant corners, in '7th International Conference on Engineering Research, Innovation and Education', Sylhet, Bangladesh.

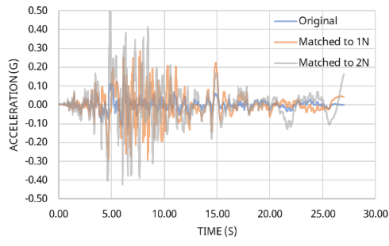
Ramalanjaona, G. (2011), 'Impact of 2004 tsunami in the islands of indian ocean: Lessons learned', *Hindawi Publishing Corporation*.

**URL:** <https://doi.org/10.1155/2011/920813>

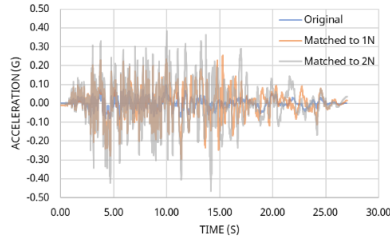
Ramdev, P., Barbude, P. R. and Patil, A. P. (2021), 'Dynamic analysis of multistory structure using linear time history analysis', *Mumbai University*.

**URL:** <https://doi.org/10.22214/ijraset.2023.53482>

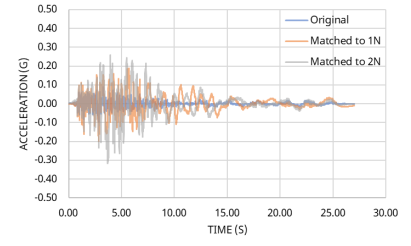
**APPENDICES**



(a) east-west

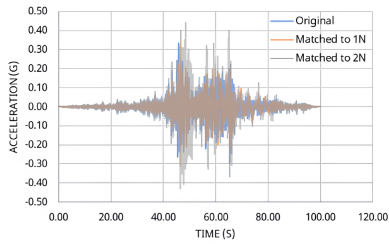


(b) north-south

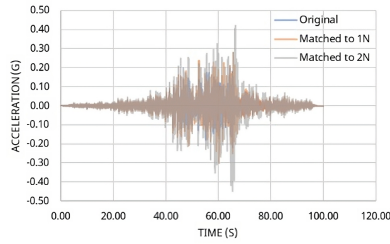


(c) vertical

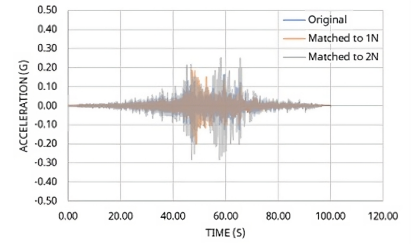
Ground motion data (unmatched, matched to 1N, and matched to 2N) of Shallow Crustal Earthquake: (a) east-west, (b) north-south, and (c) vertical.



(a) east-west

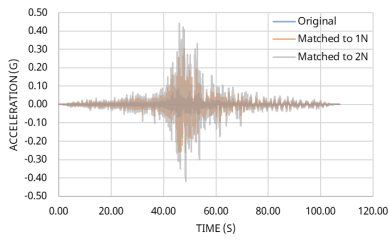


(b) north-south

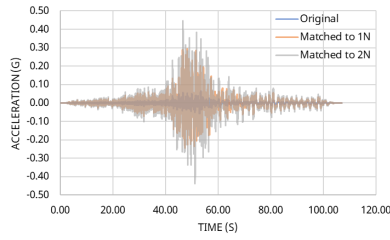


(c) vertical

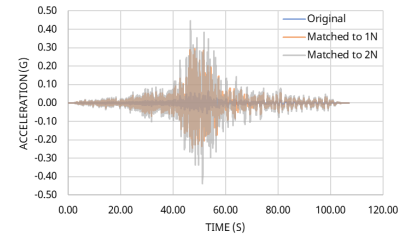
Ground motion data (unmatched, matched to 1N, and matched to 2N) of Megathrust Earthquake: (a) east-west, (b) north-south, and (c) vertical.



(a) east-west



(b) north-south



(c) vertical

Ground motion data (unmatched, matched to 1N, and matched to 2N) of Benioff Earthquake: (a) east-west, (b) north-south, and (c) vertical.